

Cosputtered composition-spread reproducibility established by high-throughput x-ray fluorescence

Cite as: J. Vac. Sci. Technol. A **28**, 1279 (2010); <https://doi.org/10.1116/1.3478668>

Submitted: 04 June 2010 . Accepted: 20 July 2010 . Published Online: 03 September 2010

John M. Gregoire, Darren Dale, Alexander Kazimirov, Francis J. DiSalvo, and R. Bruce van Dover



View Online



Export Citation

ARTICLES YOU MAY BE INTERESTED IN

[High energy x-ray diffraction/x-ray fluorescence spectroscopy for high-throughput analysis of composition spread thin films](#)

Review of Scientific Instruments **80**, 123905 (2009); <https://doi.org/10.1063/1.3274179>

[Monolithic multichannel ultraviolet detector arrays and continuous phase evolution in \$Mg_xZn_{1-x}O\$ composition spreads](#)

Journal of Applied Physics **94**, 7336 (2003); <https://doi.org/10.1063/1.1623923>

[Scanning tip microwave near-field microscope](#)

Applied Physics Letters **68**, 3506 (1996); <https://doi.org/10.1063/1.115773>



Instruments for Advanced Science

Contact Hiden Analytical for further details:
www.HidenAnalytical.com
info@hiden.co.uk

[CLICK TO VIEW](#) our product catalogue



Gas Analysis

- ▶ dynamic measurement of reaction gas streams
- ▶ catalysis and thermal analysis
- ▶ molecular beam studies
- ▶ dissolved species probes
- ▶ fermentation, environmental and ecological studies



Surface Science

- ▶ UHV/TPD
- ▶ SIMS
- ▶ end point detection in ion beam etch
- ▶ elemental imaging - surface mapping



Plasma Diagnostics

- ▶ plasma source characterization
- ▶ etch and deposition process reaction kinetic studies
- ▶ analysis of neutral and radical species



Vacuum Analysis

- ▶ partial pressure measurement and control of process gases
- ▶ reactive sputter process control
- ▶ vacuum diagnostics
- ▶ vacuum coating process monitoring



Cosputtered composition-spread reproducibility established by high-throughput x-ray fluorescence

John M. Gregoire^{a)}

Department of Materials Science and Engineering, Cornell University, Ithaca, New York 14853

Darren Dale and Alexander Kazimirov

Cornell High Energy Synchrotron Source, Cornell University, Ithaca, New York 14853

Francis J. DiSalvo

Department of Chemistry and Chemical Biology, Cornell University, Ithaca, New York 14853

R. Bruce van Dover

Department of Materials Science and Engineering, Cornell University, Ithaca, New York 14853

(Received 4 June 2010; accepted 20 July 2010; published 3 September 2010)

We describe the characterization of sputtered yttria-zirconia composition spread thin films by x-ray fluorescence (XRF). We also discuss our automated analysis of the XRF data, which was collected in a high throughput experiment at the Cornell High Energy Synchrotron Source. The results indicate that both the composition reproducibility of the library deposition and the composition measurements have a precision of better than 1 atomic percent. © 2010 American Vacuum Society. [DOI: 10.1116/1.3478668]

High throughput characterization of thin film composition spreads is an important aspect of combinatorial materials science.¹ Synchrotron-based x-ray fluorescence (XRF) experiments at 10 keV have been developed for composition mapping of inorganic libraries.^{2,3} We recently presented a combined high energy x-ray diffraction (XRD) and XRF experiment for high throughput characterization of composition spread thin films.⁴ The 60 keV x-ray energy used for this experiment was chosen for the XRD measurements, and we note that this high excitation energy enables quantitative analysis of all elements in rows 4 to 7 of the periodic table. Here, we describe the capabilities of a high throughput analysis algorithm for the XRF experiment, which provides simultaneous determination of film composition and thickness. In addition, we present the characterization of two ZrO₂-Y₂O₃ composition spread thin films prepared under the same sputter deposition conditions. The measured composition profiles for the two films coincide within 0.7 at.% over a broad range of composition, demonstrating the precision of both the synthesis and characterization techniques.

The composition-spread thin films were prepared by 90° off axis radio-frequency magnetron reactive cosputtering. Metal Zr and Y targets were placed in independently powered 2 in. magnetron sputter sources and operated in an atmosphere of 4 Pa of 40% O₂ in Ar. The Zr and Y sources were operated at 100 and 50 W, respectively. The two samples were deposited on different days and the deposition time for sample A was slightly longer than that of sample B. The 3 in. Si wafer with 500 nm SiO₂ diffusion barrier was maintained at 500 °C during deposition. The substrate was placed below and centered between the deposition sources, a geometry known to produce a deposition gradient from each source.⁵

The x-ray diffraction (XRD)/x-ray fluorescence (XRF) experiments were performed at the A2 beamline of the Cornell High Energy Synchrotron Source (CHESS). A 60 keV x-ray beam impinged on the back of the Si substrate with incident angle ~45° and 1 mm² spot size. The thin film was exposed to the direct beam on the downstream side of the substrate, and the XRF signal was obtained by a Rontec X-Flash detector oriented orthogonal to the direct beam. To preclude detection of fluorescence from other sources, a Mo and Pb shield was placed over the detector with an ~0.2 mm² hole aligned with the footprint of the beam on the thin film sample. For the ZrO₂-Y₂O₃ films, 11 substrate positions were characterized using equal-dose measurements of 6 × 10¹² photons, requiring ~250 s exposures. A flux calibration was performed through XRF analysis of a Pt film of known thickness. The XRF spectra were acquired with 2048 channels from 0 to 80 keV.

The energy-dependent detection efficiency of the experiment is shown in Fig. 1. At low energy, the efficiency is limited mainly by attenuation of the fluorescence x-rays in the 22 mm air path from sample to detector. At high energy,

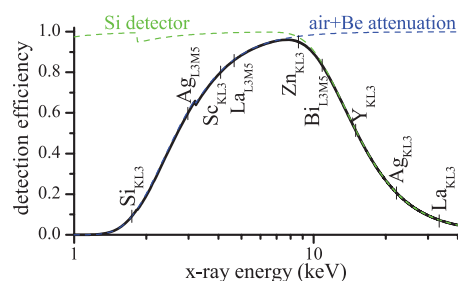


FIG. 1. (Color online) Detection efficiency of the XRF experiment with both air and Be window attenuation and detector efficiency components. To demonstrate detectability over rows 4–7 of the Periodic Table, select emission energies are noted.

^{a)}Electronic mail: jmg232@cornell.edu

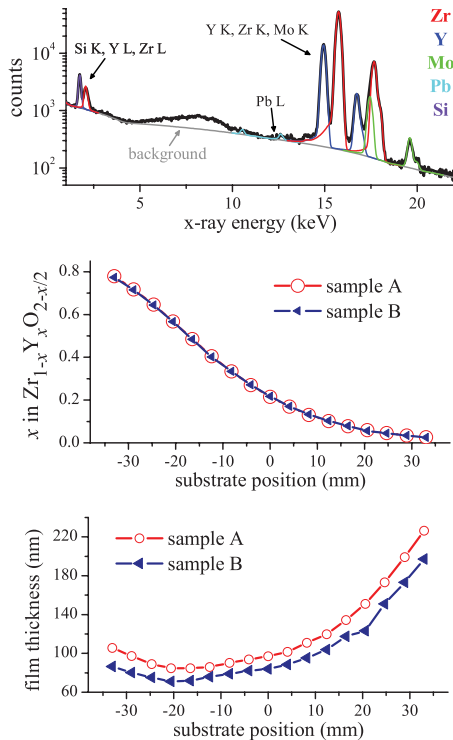


FIG. 2. (Color online) Low-energy portion of the XRF spectrum from the center position of sample A with fitted peaks (top). The Si K peak from the substrate is detected but has low intensity considering its substantial thickness (see Fig. 1). Mo and Pb are detected from excitation of the detector shroud. The Zr K and Y K fitted areas are used for quantitative analysis, providing the composition profiles (middle) and thickness profiles (bottom) for the two samples.

the efficiency is limited by absorption in the 300 μm Si detector. As indicated by the noted elemental lines, the experiment allows characterization of thin films comprising elements with atomic number Z greater than Z_K . We have successfully characterized 100 nm films with <1 wt % Sc. For $Z_{\text{Ag}} \leq Z \leq Z_{\text{La}}$ both K and L shell x-rays can be analyzed, while K (L) shell x-rays are analyzed for elements below (above) this range.

A program for automated analysis of a set of XRF spectra was developed in the PYTHON programming language using routines from the PYMCA software package.⁶ For a given spectrum, profile fitting is performed, and the resulting peak areas are used in an iterative routine to determine the film composition and thickness.

The $\text{Zr}_{1-x}\text{Y}_x\text{O}_{2-x/2}$ film was modeled as a two layer sample with the Si layer having fixed density and thickness. The thin film layer was modeled with a composition-dependent density $\rho(x) = (6.14 - 1.2x)$ g/cm³ (Ref. 7) and thickness d . Using the initial values $x = 0.5$ and $d = 100$ nm, the elemental mass fractions of Zr and Y in the thin film

layer, f_{Zr} and f_{Y} , were calculated using PYMCA. A self-consistent model of the XRF spectrum requires the sum of the calculated mass fractions to be equal to the corresponding mass fraction of the model layer:

$$f_{\text{Zr}} + f_{\text{Y}} = f_{\text{model}} \equiv \frac{(1-x)M_{\text{Zr}} + xM_{\text{Y}}}{(1-x)M_{\text{Zr}} + xM_{\text{Y}} + (2-x/2)M_{\text{O}}}, \quad (1)$$

where M is the respective atomic mass. The self-consistent solution for x and d was found by iterative PYMCA analysis by modeling the film for iteration i using $\rho_i = \rho(x_{i-1})$ and $d_i = (f_{i-1,\text{Zr}} + f_{i-1,\text{Y}} - f_{\text{model}})d_{i-1}$. Typically, the routine converges to within 10^{-4} discrepancy in mass fraction in ≤ 20 iterations.

The XRF-determined composition and thickness of two $\text{Zr}_{1-x}\text{Y}_x\text{O}_{2-x/2}$ composition-spread thin films are shown in Fig. 2. The composition profiles are essentially identical with maximum deviation in x of 0.7 at. % and mean absolute deviation of 0.1 at. %. The thickness profiles are also nearly identical with sample A measured to be $14 \pm 1.5\%$ thicker than sample B due to a corresponding difference in deposition time. The reproducibility of the $\text{Zr}_{1-x}\text{Y}_x\text{O}_{2-x/2}$ composition profile in this work indicate that both the XRF-determined compositions and cosputtered compositions have phenomenal sub-at. % precision. In this article, we do not discuss absolute accuracy or the possible introduction of systematic error in the interpretation of the XRF data. These topics are discussed in Ref. 8, where we established that this standardless XRF technique can provide ~ 3 at. % accuracy in film composition.

This material is based on the work supported as part of the Energy Materials Center at Cornell (EMC²), an Energy Frontier Research Center funded by the U.S. Department of Energy, Office of Science, Office of Basic Energy Sciences under Award No. DE-SC0001 086. This work is based on the research conducted at the Cornell High Energy Synchrotron Source (CHESS), which is supported by the National Science Foundation and the National Institutes of Health/National Institute of General Medical Sciences under NSF Award No. DMR-0225180.

¹Z. H. Barber and M. G. Blamire, *Mat. Sci. Tech.* **24**, 757 (2008).

²S. Vogt, Y. Chu, A. Tkachuk, P. Ilinski, D. Walko, and F. Tsui, *Appl. Surf. Sci.* **223**, 214 (2004).

³B. Xia, Y. S. Chu, and W. L. Gladfelter, *Surf. Coat. Technol.* **201**, 9041 (2007).

⁴J. M. Gregoire, D. Dale, A. Kazimirov, F. J. DiSalvo, and R. B. van Dover, *Rev. Sci. Instrum.* **80**, 123905 (2009).

⁵R. B. van Dover and L. F. Schneemeyer, *Macromol. Rapid Commun.* **25**, 150 (2004).

⁶V. Solé, E. Papillon, M. Cotte, P. Walter, and J. Susini, *Spectrochim. Acta* **B62**, 63 (2007).

⁷JCPDS Card Nos. 4-010-3273 and 30-1468.

⁸J. M. Gregoire, D. Dale, A. Kazimirov, F. J. DiSalvo, and R. B. van Dover, *Rev. Sci. Instrum.* **80**, 123905 (2009).